# Journal of Materials Chemistry A

Accepted Manuscript


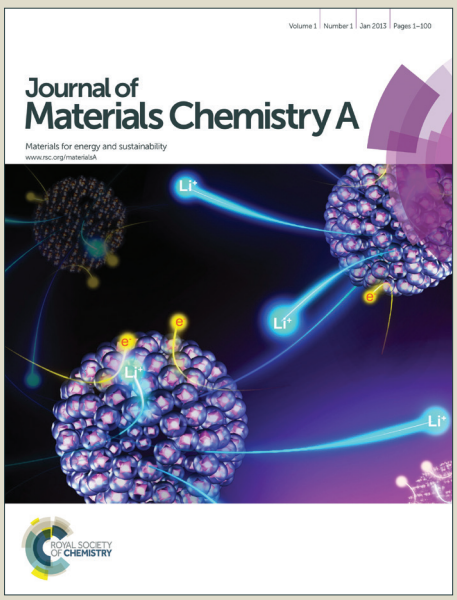





ROYAL SOCIETY OF CHEMISTRY

www.rsc.org/materialsA

# Low-cost solution-processed copper iodide as an alternative to PEDOT: PSS hole transport layer for efficient and stable inverted planar heterojunction perovskite solar cells

Wei-Yi Chen,[a] Lin-Long Deng,*[a] Si-Min Dai,[b] Xin Wang,[a] Cheng-Bo Tian,[b] Xin-Xing Zhan,[b] Su-Yuan Xie,*[b] Rong-Bin Huang[b] and Lan-Sun Zheng[b]

[a]*Pen-Tung Sah Institute of Micro-Nano Science and Technology, Xiamen University, Xiamen 361005, China. E-mail: denglinlong@xmu.edu.cn*

[b]*State Key Lab for Physical Chemistry of Solid Surfaces, iChEM (Collaborative Innovation Center of Chemistry for Energy Materials), Department of Chemistry, College of Chemistry and Chemical Engineering, Xiamen University, Xiamen 361005, China. E-mail: syxie@xmu.edu.cn*

Inverted planar heterojunction (PHJ) perovskite solar cells have attracted great attention due to their advantages of low-temperature fabrication on flexible substrates by solution processing with high efficiency. Poly(3,4-ethylenedioxythiophene): polystyrenesulfonate (PEDOT:PSS) is the most widely used hole transport layer (HTL) in inverted PHJ perovskite solar cells; however, the acidic and hygroscopic nature of PEDOT: PSS can cause degradation and reduce the device stability. In this work, we demonstrated that low-cost solution-processed hydrophobic copper iodide (CuI) can serve as a HTL to replace PEDOT: PSS in inverted PHJ perovskite solar cells with high performance and enhanced device stability. Power conversion efficiency (PCE) of 13.58% was achieved by employing CuI as a HTL, slightly exceeding PEDOT: PSS based device with PCE of 13.28% under the same experimental conditions. Furthermore, the CuI based devices exhibited better air stability than that of PEDOT: PSS based devices. The results indicate that low-cost solution-processed CuI is a promising alternative to PEDOT: PSS HTL and could be widely used in inverted PHJ perovskite solar cells.

## Introduction

Organic-inorganic hybrid perovskites have received tremendous attention as a promising candidate for developing next-generation photovoltaic cells because of their advantages such as broad light absorption,[1, 2] direct bandgap,[3] high charge-carrier mobility,[4] long exciton diffusion length,[5, 6] and solution processability.[7, 8] Owing to these merits, perovskite solar cells have made

significant progress in recent years, with power conversion efficiencies (PCEs) boosted from 3.8% up to over 20%.[1, 9-13] Conventional perovskite solar cells are typically fabricated using titanium oxide (or other metal oxide) as the electron transport layer (ETL) and 2,2'-7,7'-tetrakis(*N*,*N*-di-*p*-methoxyphenylamine)-9,9'-spirobifluorene (spiro-OMeTAD) as the hole transport layer (HTL). However, the high processing temperature of titanium oxide and the relatively high cost of spiro-OMeTAD limit the further development of perovskite solar cells, especially in flexible substrates. To overcome these drawbacks, inverted planar heterojunction (PHJ) perovskite solar cells[14-18] using poly(3,4-ethylenedioxythiophene): poly(styrenesulfonate) (PEDOT: PSS) as the HTL and a fullerene derivative [6,6]-phenyl-$C_{61}$-butyric acid methylester (PCBM) as the ETL have been developed and demonstrated promising efficiencies over 18%.[19, 20]

Inverted PHJ perovskite solar cells are becoming popular because they can be fabricated on flexible substrates with simple device structure and low-temperature solution processing. In inverted PHJ perovskite solar cells, PEDOT: PSS is the most widely used HTL due to its high conductivity, high transparency and high work function.[14-18] However, the acidic and hygroscopic nature of PEDOT: PSS could cause degradation and reduce the device stability.[21-25] Inorganic *p*-type semiconductors such as nickel oxide ($NiO_x$)[23, 26, 27] or copper-doped $NiO_x$[24] have been explored in replacing PEDOT: PSS to avoid its acidic and hygroscopic characteristics. Nevertheless, the potential health risk of nickel oxide[28-33] could hinder its widespread adoption in perovskite solar cells.

Inorganic copper-based *p*-type semiconductors such as copper iodide (CuI) and copper thiocyanate (CuSCN), have also attracted great attention due to their large bandgap, high conductivity, low cost and solution processibility, and they have been widely used as HTLs in organic solar cells,[34, 35] dye-sensitized solar cells,[36-38] and perovskite solar cells.[27, 39, 40] Although doctor-bladed CuI has been used in conventional perovskite solar cells to replace spiro-OMeTAD, the relatively low PCE of 6.0%[40] result from low open-circuit voltage ($V_{oc}$) suggests that there is still much room for improvement in performance. Electrodeposited CuSCN has also been employed as HTL in inverted planar perovskite solar cells; however, the high series resistance of the CuSCN films lead to very low PCE of 3.8%.[27] In spite of relatively low efficiency, the low-cost and decent air stability of copper-based inorganic HTLs make them potentially feasible

replacements for the organic HTLs in perovskite solar cells, which represent a promising step toward further development.

In this work, we demonstrated that low-cost solution-processed CuI can serve as a HTL to replace the commonly used PEDOT: PSS in inverted PHJ perovskite solar cells with high performance and enhanced stability. A solution-processed device with the structure of FTO/CuI/$CH_3NH_3PbI_3$/PCBM/Al showed a $V_{oc}$ of 1.04 V, a short-circuit current density ($J_{sc}$) of 21.06 mA/cm$^2$, and a PCE of 13.58% under standard AM 1.5G simulated solar irradiation, while the device with PEDOT: PSS as a HTL displayed a $V_{oc}$ of 0.93 V, a $J_{sc}$ of 19.36 mA/cm$^2$, and a PCE of 13.28% under the same experimental conditions. The results indicate that low-cost solution-processed CuI is an alternative to PEDOT: PSS HTL and could be widely used in inverted PHJ perovskite solar cells.

## Experimental Section

### Materials and preparation

$PbI_2$ (99.9985%), CuI (99.998%) were purchased from Alfa Aesar. *N*,*N*-dimethylformamide (DMF) (99.8%), and acetonitrile (99.8%) were received from Sigma-Aldrich. PCBM were purchased from American Dye Source Inc. Methylammonium iodide ($CH_3NH_3I$) was synthesized following a previously reported method.[41]

### Device fabrication and characterization

Perovskite solar cells with the configuration of FTO/PEDOT: PSS (or CuI)/ $CH_3NH_3PbI_3$/ PCBM/Al were fabricated. Patterned FTO glass substrates were cleaned sequentially with detergent, deionized water, acetone, and isopropyl alcohol followed by drying with $N_2$ flow and UV-ozone treatment for 10 min. Then different hole transport layers (PEDOT: PSS, and CuI) were formed by spin-coating on the substrates. The PEDOT: PSS solution (Baytron P VP AI 4083) was filtered and spin-coated onto the cleaned FTO substrates at 2000 rpm for 30 s, and baked at 150 $^oC$ for 20 min in air. The CuI films were prepared by spin-coating copper iodide acetonitrile solution (10 mg/mL) at 4000 rpm for 30 s in the glove box, and baked on the hot plate at 100 $^oC$ for 10 min. Then solution of 1M $PbI_2$ in DMF was first spin coated on top of the prepared substrates at 5000 rpm for 30 s, then baked at 70 $^oC$ for 10 min, and subsequently converted to $CH_3NH_3PbI_3$ by a gas-solid crystallization process with some modification.[42] The gas-solid crystallization process

was carried out in a closed container, in which the FTO/PEDOT: PSS (or CuI)/$PbI_2$ substrates were placed with the $PbI_2$ side facing down at a constant height of around 2 in. against the $CH_3NH_3I$ powder (~50mg). The container was putted into a vacuum oven at a vacuum degree of ~133 Pa, and then heated at 150 $^oC$ for desired time. The optimized reaction time is 3 h, and 2 h for FTO/PEDOT:PSS/$PbI_2$ substrates, and FTO/CuI/$PbI_2$ substrates, respectively. After the $CH_3NH_3PbI_3$ film was formed and then cooled to room temperature, 2 wt% PCBM in chlorobenzene was spin-coated onto the $CH_3NH_3PbI_3$ layer at 2000 rpm for 30 s. Finally, Al electrode (~100 nm) was deposited by thermal evaporation under a vacuum of ~$2\times10^{-4}$ Pa through a shadow mask. The area of device is ~0.06 $cm^2$ for each solar cell discussed in this work.

The photovoltaic performance was measured in air without any encapsulation under an AM 1.5G filter at 100 $mW/cm^2$ using a Newport Oriel 92192 Solar Simulator, as calibrated by a standard Si solar cell. The current density-voltage (*J-V*) characteristics were measured using a Keithley 2420 source meter. The external quantum efficiency (EQE) was measured using a Newport Oriel QE/IPCE measurement kit. The light intensity was calibrated using a single-crystal Si photovoltaic cell as a reference. UV-Vis absorption spectra were measured on a Varian Cary 5000 UV-Vis-NIR spectrometer. Atomic force microscopy (AFM) images were obtained by using a Pico SPM instrument (Molecular Imaging Co., USA) operated in tapping mode. The scanning electron microscope (SEM) images were taken on a ZEISS Sigma FE-SEM. The X-ray diffraction (XRD) patterns were recorded on a Rigaku Ultima IV diffractometer using Cu K$\alpha$ radiation. The thickness of the thin films was measured by using a KLA-Tencor Alpha Step D-100 Stylus Profiler.

## Results and discussion

### CuI thin film characterization

The transmission spectra of PEDOT: PSS film and CuI film on quartz substrates are shown in Fig. 1. The thickness values are similar between PEDOT: PSS film (~40 nm) and CuI film (~43 nm). Both films were highly transparent in the visible range from 400 to 800 nm. Moreover, the CuI film exhibited slightly higher transmittance than that of PEDOT: PSS film from 450 to 800 nm. It should be noted that an obvious hump at about 407 nm was observed in CuI film, which may be due to the excitation of electrons from sub-bands in the valence band to the conduction band of

CuI.[43] The high transparency of CuI film makes it beneficial to use as HTL because it could allow more photo flux to reach light absorbing layer for generating photocurrent.

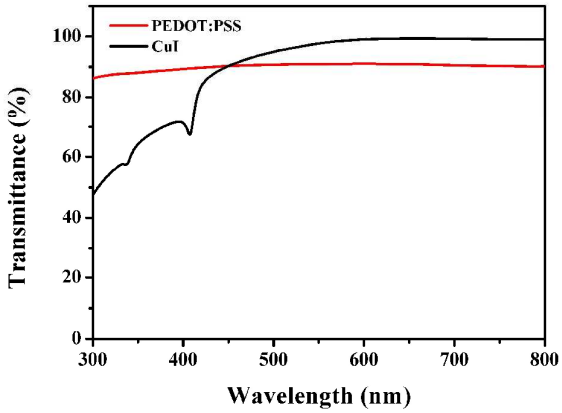


**Fig. 1** Optical transmission spectra of PEDOT: PSS film and CuI film on quartz substrates.

CuI is a wide bandgap (3.1 eV) semiconductor with three crystalline phases $\alpha$, $\beta$ and $\gamma$. Among the three crystalline phases, $\gamma$-phase CuI behaves as a *p*-type semiconductor.[44] The X-ray diffraction (XRD) patterns of CuI films on FTO glass substrates are displayed in Fig. 2. For comparison, the XRD spectra of the FTO substrates, FTO/PEDOT: PSS substrates, as well as the $PbI_2$ films and $CH_3NH_3PbI_3$ films on both FTO/PEDOT: PSS and FTO/CuI substrates are also given. The FTO substrates showed strong diffraction peaks at 26.36°, 33.57°, 37.60°, 51.38°, 54.55°, 61.40°, and 65.39°, which can be assigned to the (110), (101), (200), (211), (220), (310), and (301) planes of FTO.[45] The diffraction peaks of FTO/PEDOT: PSS substrates are nearly identical to those of FTO substrates because of the amorphous nature of PEDOT: PSS layer.[46] By contrast, the CuI films exhibited an intense peak at 25.46° corresponding to the (111) reflection of polycrystalline $\gamma$-phase copper iodide with a zinc-blende face centered cubic structure.[47] The $PbI_2$ films spin-coated on both FTO/PEDOT: PSS and FTO/CuI substrates showed almost the same diffraction peaks at 12.65°, 25.50°, 38.58°, and 52.36°, corresponding to (001), (002), (003), and (004) planes of $PbI_2$, which indicates the preferential crystal growth orientation along the *c* axis.[9] The existence of *p*-type $\gamma$-phase CuI thin film deposited on FTO substrate as confirmed by XRD results, along with its valance band compared to $CH_3NH_3PbI_3$,[2] makes it possible to employ CuI as HTL in perovskite solar cells.

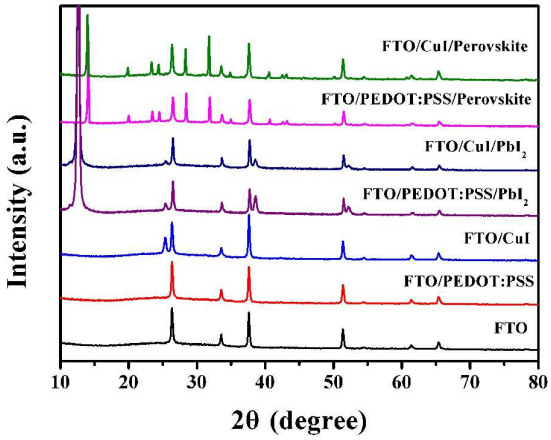


**Fig. 2** XRD patterns of FTO, FTO/PEDOT:PSS, FTO/CuI, FTO/PEDOT:PSS/$PbI_2$, FTO/CuI/$PbI_2$, FTO/PEDOT:PSS/$CH_3NH_3PbI_3$, and FTO/CuI/$CH_3NH_3PbI_3$ on glass substrates.

Photoluminescence (PL) measurements were conducted to investigate if CuI film can efficiently extract photo-generated carries from perovskite absorber and be employed as HTL in perovskite solar cells. The carrier extraction efficiency of PEDOT: PSS film was also measured for comparison. As shown in Fig. 3, a significant quenching effect was observed when the perovskite layer contacts with either CuI or PEDOT: PSS layer. Moreover, the CuI film exhibits PL quenching more efficiently than that of PEDOT: PSS film, which demonstrates that CuI can be used as HTL in replacing PEDOT: PSS for high performance perovskite solar cells.

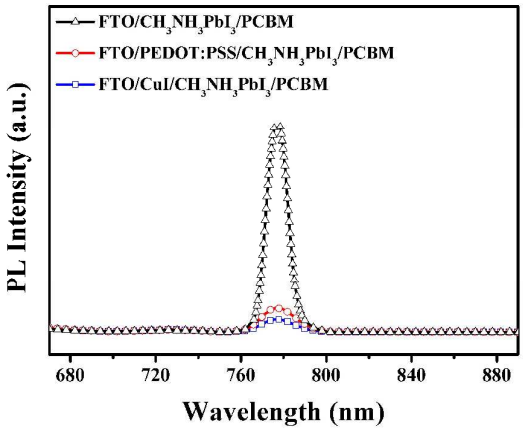


**Fig. 3** Photoluminescence spectra (excited at 600 nm) of $CH_3NH_3PbI_3$/PCBM, PEDOT: PSS/ $CH_3NH_3PbI_3$/PCBM, and CuI/$CH_3NH_3PbI_3$/PCBM on FTO glass substrates.

To understand the influence of interfacial layers on device performance, the morphologies of the different buffer layers were observed by AFM and SEM. The surface topographies of FTO, FTO/PEDOT: PSS, and FTO/CuI were determined by atomic force microscope (AFM) as shown in Fig. 4(a)-4(c). The root mean square (RMS) roughness of bare FTO was 6.3 nm, while the RMS roughness decreased to 3.4 nm after being covered with PEDOT: PSS layer. In contrast, the RMS roughness increased to 8.6 nm after being covered with CuI layer, which may be due to the formation of large CuI grains. SEM images of the FTO, FTO/PEDOT: PSS, and FTO/CuI were also shown in Fig. 4(d)-4(f). As shown in Fig. 4(e), the PEDOT: PSS film exhibited a highly smooth surface and covered the FTO completely. By comparison, the CuI film showed a rough surface with large CuI grains, which indicates the polycrystalline character of CuI film that correlates well with the XRD result.

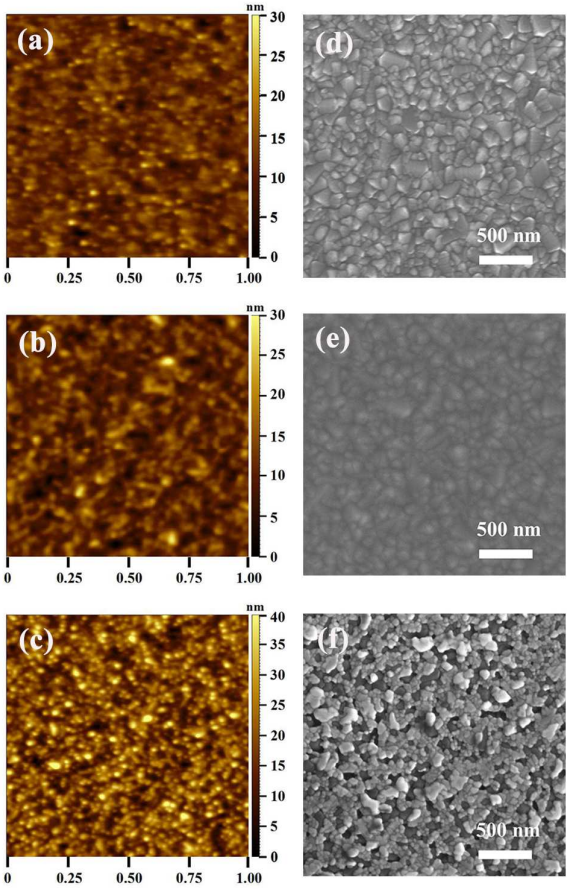

**Fig. 4** AFM topography and SEM images of FTO (a, d), FTO/PEDOT: PSS (b, e) and FTO/CuI (c, f).

**Fabrication and Characterization of Perovskite Solar Cells**

Based on these results, inverted PHJ perovskite solar cells with the configuration: FTO/PEDOT: PSS (or CuI)/$CH_3NH_3PbI_3$/PCBM/Al (Fig. 5(a)) were fabricated, using PEDOT: PSS or CuI as the HTL (cross-sectional SEM images are shown in ESI Fig. S1†). According to the previous reports,[34] the HOMO (or valence band) of CuI was estimated to be -5.1 eV, which is slighter lower than that of PEDOT: PSS (-5.0 eV) and matched well with the energy levels of $CH_3NH_3PbI_3$,[2] indicating that both of they can be used as suitable HTLs for pervoskite solar cells. Together with $PC_{61}BM$ and Al electrode, the energy level alignment was depicted in Fig. 5(b).[18] A thin layer (~40 nm) of PEDOT: PSS or CuI film was deposited on the FTO substrates by spin-coating. After thermal annealing, the $CH_3NH_3PbI_3$ film was prepared via a two-step gas-solid crystallization process according to the procedure reported in the literature.[42] The composition and morphology of the $CH_3NH_3PbI_3$ films were investigated by X-ray diffraction (XRD) and scanning electron microscopy (SEM) measurements. As shown in Fig. 2, the XRD peak positions for $CH_3NH_3PbI_3$ films on both PEDOT: PSS and CuI substrates are almost the same. The diffraction peaks at 14.10°, 20.01°, 23.48°, 24.50°, 28.45°, 31.89°, 34.98°, 40.68°, 42.59°, 43.20°, and 50.22° correspond to planes (110), (112), (211), (202), (220), (310), (312), (224), (411), (314), and (404) of the $CH_3NH_3PbI_3$ tetragonal phase, indicating the fully formation of perovskite structure from $PbI_2$.[9, 48, 49] The as-formed $CH_3NH_3PbI_3$ films grown on both PEDOT: PSS and CuI substrates exhibit full surface coverage and are composed of micrometer-sized grains (see ESI Fig. S2†). Therefore, the full surface coverage, microscale grain size, and uniform grain structure of the as-formed perovskite films on both PEDOT: PSS and CuI substrates are highly suitable for inverted PHJ perovskite solar cells.

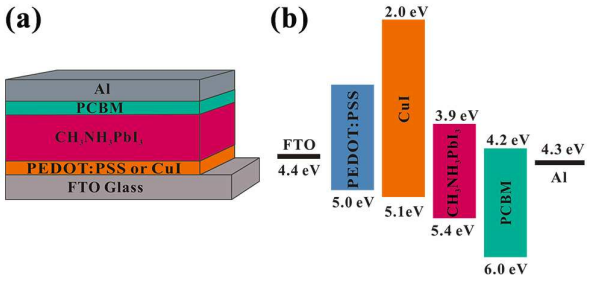


**Fig. 5** Device structure of inverted PHJ perovskite solar cell (a), and energy level alignment of various device layers (b).

**Photovoltaic Performance of Perovskite Solar Cells**

The current density-voltage (*J-V*) characteristics of inverted PHJ perovskite solar cells employing PEDOT: PSS and CuI as the HTLs under AM 1.5 G conditions (100 mWcm$^{-2}$) are shown in Fig. 6(a) and the relevant parameters are summarized in Table 1. A reference cell without any HTL was prepared for comparison, which displayed a $V_{oc}$ of 0.90 V, a $J_{sc}$ of 15.22 mA/cm$^2$, and a FF of 40.6 %, resulting in a PCE of 5.56%. Employing PEDOT: PSS and CuI as HTLs substantially increased the PCE of the best devices to 13.28% for PEDOT: PSS and 13.58% for CuI. The overall efficiency enhancement mainly came from a significant increase in FF and $J_{sc}$ values, while the $V_{oc}$ values only marginally varied. The device with PEDOT: PSS as the HTL displayed a $V_{oc}$ of 0.93 V, a $J_{sc}$ of 19.36 mA/cm$^2$, a FF of 73.8 %, and a PCE of 13.28%. By contrast, employing CuI as the HTL slightly improves device performance, particularly $V_{oc}$ and $J_{sc}$, as a consequence, the PCE reached 13.58%, which is slightly higher than that of PEDOT: PSS based device. The ~0.1 V higher $V_{oc}$ for CuI compared to PEDOT: PSS comes from the lower HOMO energy level and the higher $J_{sc}$ mainly due to more efficient charge transport process and/or light harvesting. However, the decrease in FF for CuI reflects the lower shunt resistance ($R_{sh}$), which may be due to some leakage paths.[34, 50] As shown by SEM study, the FTO electrode was entirely covered with PEDOT: PSS, however, it was not completely covered by CuI. The imperfect coverage of CuI on the FTO substrate may form some leakage paths from FTO to the perovskite absorbing layer. Moreover, the leakage paths can also be confirmed by AFM study. As shown in Fig. 4, small islands were observed in CuI layer, and they could influence the perovskite layer and thus cause large leakage current and small $R_{sh}$.

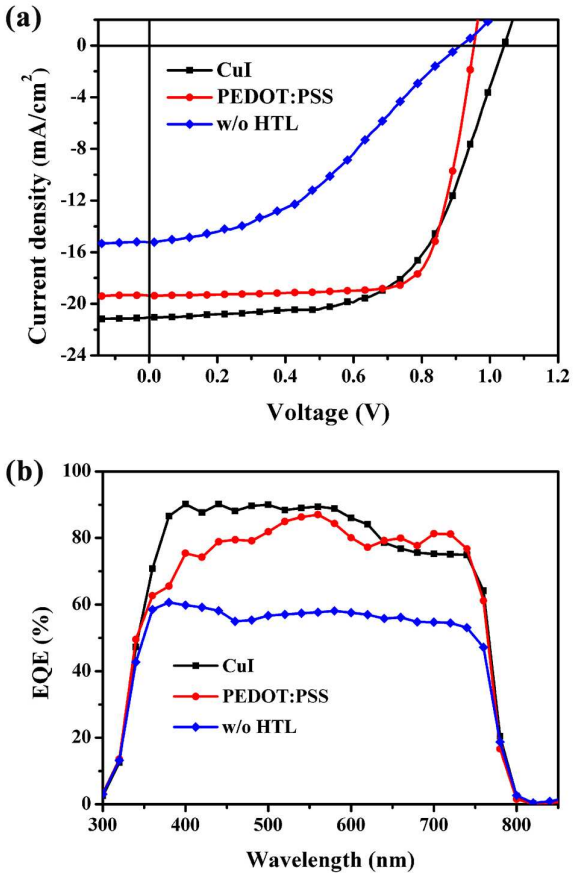


**Fig. 6** *J-V* curves (a) and EQE spectra (b) for perovskite solar cells fabricated by using PEDOT: PSS and CuI as HTL, and a reference cell without HTL.

**Table 1** Photovoltaic parameters of perovskite solar cells with different HTLs

| HTL | $V_{oc}$ (V) | $J_{sc}$ (mA/cm$^2$) | FF (%) | PCE (%) |
|---|---|---|---|---|
| CuI | 1.04 | 21.06 | 62.0 | 13.58 |
| PEDOT:PSS | 0.93 | 19.36 | 73.8 | 13.28 |
| w/o HTL | 0.90 | 15.22 | 40.6 | 5.56 |

The external quantum efficiency (EQE) spectra for perovskite solar cells using PEDOT: PSS or CuI as the HTL and without HTL are shown in Fig. 6(b). The use of PEDOT: PSS and CuI as HTLs significantly improved the photocurrent in region from 400 to 800 nm due to more effective charge extraction, which is correlated well with the more effective PL quench of PEDOT: PSS and

CuI as shown in Fig. 3. Interestingly, the EQE curve shape of the device using CuI as HTL differed from that of the device employing PEDOT: PSS as HTL. This phenomenon may be attributed to the distinct differences in light absorption and interference effect between CuI and PEDOT: PSS. The integrated current densities from the EQE spectra for devices using PEDOT: PSS and CuI as HTL and without HTL is 18.79, 20.36, and 14.85 mA/cm$^2$, respectively, which is in good agreement with the corresponding $J_{sc}$ obtained from the *J-V* curves.

To study the hysteresis effects of devices incorporating PEDOT: PSS or CuI as the HTL, both forward and reverse scan directions were conducted. Both PEDOT: PSS and CuI based devices exhibited relatively consistent PCEs under different scan directions (ESI Fig. S3†), which indicate slight hysteresis effect in the inverted PHJ perovskite solar cells incorporating PEDOT: PSS or CuI as the HTL.

**Stability of Perovskite Solar Cells**

The long-term stability of perovskite solar cells is of vital importance for practical applications. Although PEDOT: PSS has been widely used as a HTL in high performance inverted PHJ PSCs; the acidic and hygroscopic characteristics of PEDOT: PSS is unfavorable for device stability.[21-25] In this respect, the hydrophobic nature and excellent ambient stability of CuI are advantageous for solar cell application.[34, 51] To verify this, the air stability of perovskite solar cells without encapsulation was characterized and is exhibited in Fig. 7. Since Al electrode could be severely corroded by decomposition of perovskite film after air exposure and thereby potentially affect the device stability,[25] silver was used as the top electrode instead of aluminum to avoid degeneration induced by top electrode. As shown in Fig. 7, device using CuI as HTL shows improved air stability as compared to device employing PEDOT: PSS as HTL. The CuI-based device maintained 90% of its initial efficiency after 14 days storage in air, while the PEDOT: PSS-based device retained only 27% after 14 days, which was mainly due to gradual decrease in $J_{sc}$ and FF. The lower stability of PEDOT: PSS-based device maybe result from the acidic and hygroscopic nature of PEDOT: PSS as well as the moisture-sensitive perovskite layer.[22, 24, 25]

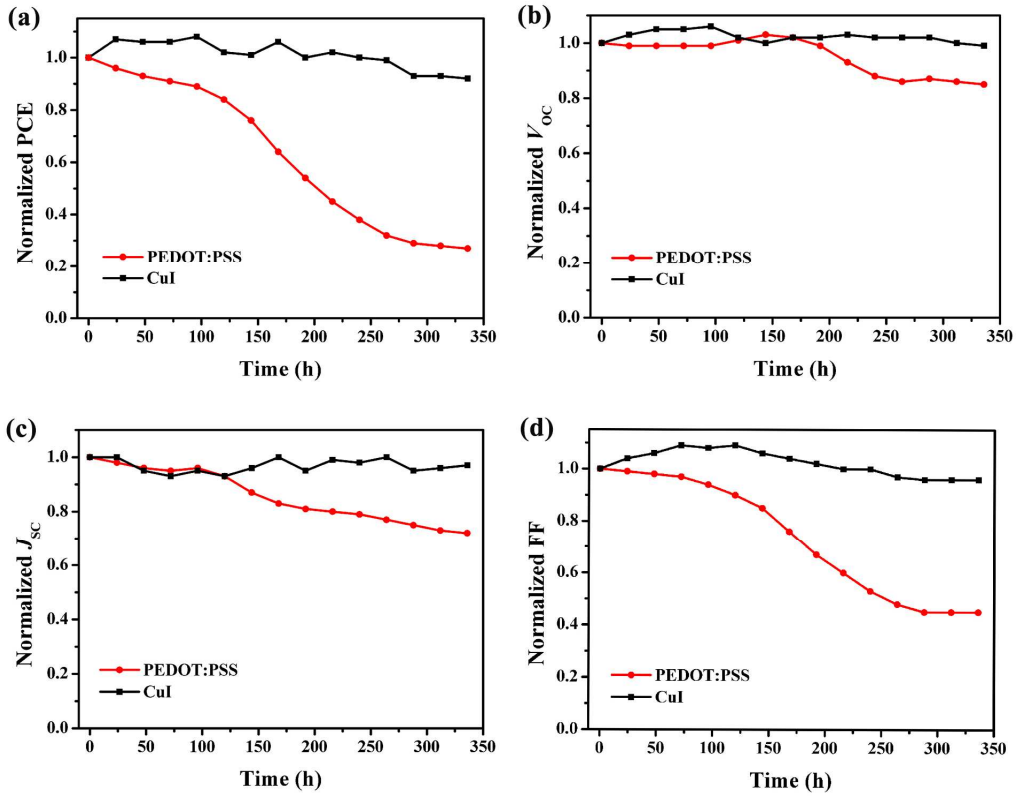


**Fig. 7** Normalized PCE (a), $V_{oc}$ (b), $J_{sc}$ (c), and FF (d) of perovskite solar cells empolying PEDOT: PSS and CuI HTL as a function of storage time in air.

## Conclusions

In conclusion, we demonstrated that low-cost solution-processed CuI is a promising HTL for high efficient and stable inverted PHJ perovskite solar cells. Benefiting from high transmittance and deep valance band of CuI, devices employing CuI as HTL exhibit higher $V_{oc}$ and $J_{sc}$ than devices using PEDOT: PSS as HTL. As a result, CuI based devices exhibited slightly higher efficiency than that of PEDOT: PSS based devices. Furthermore, the hydrophobic nature and excellent ambient stability of CuI dramatically enhanced the stability of inverted PHJ perovskite solar cells. This work reveals that low-cost solution-processed CuI is an alternative to PEDOT: PSS and could be widely used in inverted PHJ perovskite solar cells with high performance and stability.

## Acknowledgements

The authors sincerely acknowledge Prof. Bing-Wei Mao for her help in AFM measurement. This work was supported by the National Basic Research 973 Program of China (2011CB935901, and 2014CB845601), the National Nature Science Foundation of China (U1205111, 21390390, 21031004, 21021061, J1210014, and 20923004), and the Fundamental Research Funds for the Central Universities (20720140512).

## References

1 A. Kojima, K. Teshima, Y. Shirai and T. Miyasaka, *J. Am. Chem. Soc.*, 2009, **131**, 6050.
2 H.-S. Kim, C.-R. Lee, J.-H. Im, K.-B. Lee, T. Moehl, A. Marchioro, S.-J. Moon, R. Humphry-Baker, J.-H. Yum, J. E. Moser, M. Grätzel and N.-G. Park, *Sci. Rep.*, 2012, **2**, 591.
3 W.-J. Yin, J.-H. Yang, J. Kang, Y. Yan and S.-H. Wei, *J. Mater. Chem. A*, 2015, **3**, 8926.
4 C. Wehrenfennig, G. E. Eperon, M. B. Johnston, H. J. Snaith and L. M. Herz, *Adv. Mater.*, 2014, **26**, 1584.
5 D. Stranks Samuel, E. Eperon Giles, G. Grancini, C. Menelaou, J. P. Alcocer Marcelo, T. Leijtens, M. Herz Laura, A. Petrozza and J. Snaith Henry, *Science*, 2013, **342**, 341.
6 G. Xing, N. Mathews, S. Sun, S. S. Lim, Y. M. Lam, M. Grätzel, S. Mhaisalkar and T. C. Sum, *Science*, 2013, **342**, 344.
7 M. M. Lee, J. Teuscher, T. Miyasaka, T. N. Murakami and H. J. Snaith, *Science*, 2012, **338**, 643.
8 M. Liu, M. B. Johnston and H. J. Snaith, *Nature*, 2013, **501**, 395.
9 J. Burschka, N. Pellet, S.-J. Moon, R. Humphry-Baker, P. Gao, M. K. Nazeeruddin and M. Grätzel, *Nature*, 2013, **499**, 316.
10 D. Liu and T. L. Kelly, *Nat. Photonics*, 2014, **8**, 133.
11 Y.-J. Jeon, S. Lee, R. Kang, J.-E. Kim, J.-S. Yeo, S.-H. Lee, S.-S. Kim, J.-M. Yun and D.-Y. Kim, *Sci. Rep.*, 2014, **4**, 6953.
12 H. Zhou, Q. Chen, G. Li, S. Luo, T.-b. Song, H.-S. Duan, Z. Hong, J. You, Y. Liu and Y. Yang, *Science*, 2014, **345**, 542.
13 S. Yang Woon, H. Noh Jun, J. Jeon Nam, C. Kim Young, S. Ryu, J. Seo and I. Seok Sang, *Science*, 2015, **348**, 1234.
14 J.-Y. Jeng, Y.-F. Chiang, M.-H. Lee, S.-R. Peng, T.-F. Guo, P. Chen and T.-C. Wen, *Adv. Mater.*, 2013, **25**, 3727.
15 P. Docampo, J. M. Ball, M. Darwich, G. E. Eperon and H. J. Snaith, *Nat. Commun.*, 2013, **4**, 3761.
16 S. Sun, T. Salim, N. Mathews, M. Duchamp, C. Boothroyd, G. Xing, T. C. Sum and Y. M. Lam, *Energy Environ. Sci.*, 2014, **7**, 399.
17 J. You, Z. Hong, Y. Yang, Q. Chen, M. Cai, T.-B. Song, C.-C. Chen, S. Lu, Y. Liu and H. Zhou, *ACS Nano*, 2014, **8**, 1674.
18 J. Seo, S. Park, Y. Chan Kim, N. J. Jeon, J. H. Noh, S. C. Yoon and S. I. Seok, *Energy Environ. Sci.*, 2014, **7**, 2642.
19 W. Nie, H. Tsai, R. Asadpour, J.-C. Blancon, A. J. Neukirch, G. Gupta, J. J. Crochet, M. Chhowalla, S. Tretiak, M. A. Alam, H.-L. Wang and A. D. Mohite, *Science*, 2015, **347**, 522.

20 J. H. Heo, H. J. Han, D. Kim, T. K. Ahn and S. H. Im, *Energy Environ. Sci.*, 2015, **8**, 1602.

21 M. P. de Jong, L. J. van Ijzendoorn and M. J. A. de Voigt, *Appl. Phys. Lett.*, 2000, **77**, 2255.

22 M. Joergensen, K. Norrman and F. C. Krebs, *Sol. Energy Mater. Sol. Cells*, 2008, **92**, 686.

23 J.-Y. Jeng, K.-C. Chen, T.-Y. Chiang, P.-Y. Lin, T.-D. Tsai, Y.-C. Chang, T.-F. Guo, P. Chen, T.-C. Wen and Y.-J. Hsu, *Adv. Mater.* , 2014, **26**, 4107.

24 J. H. Kim, P.-W. Liang, S. T. Williams, N. Cho, C.-C. Chueh, M. S. Glaz, D. S. Ginger and A. K. Y. Jen, *Adv. Mater.*, 2015, **27**, 695.

25 H. Choi, C.-K. Mai, C. Bazan Guillermo, J. Heeger Alan, H.-B. Kim, J. Jeong, S. Song and Y. Kim Jin, *Nat. Commun.*, 2015, **6**, 7348.

26 K.-C. Wang, P.-S. Shen, M.-H. Li, S. Chen, M.-W. Lin, P. Chen and T.-F. Guo, *ACS Appl. Mater. Interfaces*, 2014, **6**, 11851.

27 A. S. Subbiah, A. Halder, S. Ghosh, N. Mahuli, G. Hodes and S. K. Sarkar, *J. Phys. Chem. Lett.*, 2014, **5**, 1748.

28 J. K. Dunnick, M. R. Elwell, A. E. Radovsky, J. M. Benson, F. F. Hahn, K. J. Nikula, E. B. Barr and C. H. Hobbs, *Cancer Res.*, 1995, **55**, 5251.

29 E. Denkhaus and K. Salnikow, *Crit Rev Oncol Hematol*, 2002, **42**, 35.

30 S. Kawanishi, S. Oikawa, S. Inoue and K. Nishino, *Environ. Health Perspect. Suppl.*, 2002, **110**, 789.

31 M. Cempel and G. Nikel, *Pol. J. Environ. Stud.*, 2006, **15**, 375.

32 M. Horie, K. Nishio, K. Fujita, H. Kato, A. Nakamura, S. Kinugasa, S. Endoh, A. Miyauchi, K. Yamamoto, H. Murayama, E. Niki, H. Iwahashi, Y. Yoshida and J. Nakanishi, *Chem. Res. Toxicol.*, 2009, **22**, 1415.

33 A. Munoz and M. Costa, *Toxicol. Appl. Pharmacol.*, 2012, **260**, 1.

34 W. Sun, H. Peng, Y. Li, W. Yan, Z. Liu, Z. Bian and C. Huang, *J. Phys. Chem. C*, 2014, **118**, 16806.

35 S. Das, J.-Y. Choi and T. L. Alford, *Sol. Energy Mater. Sol. Cells*, 2015, **133**, 255.

36 V. P. S. Perera and K. Tennakone, *Sol. Energy Mater. Sol. Cells*, 2003, **79**, 249.

37 M. Rusop, T. Shirata, P. M. Sirimanne, T. Soga, T. Jimbo and M. Umeno, *Appl. Surf. Sci.*, 2006, **252**, 7389.

38 J.-H. Yum, P. Chen, M. Grätzel and M. K. Nazeruddin, *ChemSusChem*, 2008, **1**, 699.

39 P. Qin, S. Tanaka, S. Ito, N. Tetreault, K. Manabe, H. Nishino, M. K. Nazeeruddin and M. Grätzel, *Nat. Commun.*, 2014, **5**, 3834.

40 J. A. Christians, R. C. M. Fung and P. V. Kamat, *J. Am. Chem. Soc.*, 2014, **136**, 758.

41 L. Etgar, P. Gao, Z. Xue, Q. Peng, A. K. Chandiran, B. Liu, M. K. Nazeeruddin and M. Grätzel, *J. Am. Chem. Soc.*, 2012, **134**, 17396.

42 F. Hao, C. C. Stoumpos, Z. Liu, R. P. H. Chang and M. G. Kanatzidis, *J. Am. Chem. Soc.*, 2014, **136**, 16411.

43 P. M. Sirimanne, M. Rusop, T. Shirata, T. Soga and T. Jimbo, *Chem. Phys. Lett.*, 2002, **366**, 485.

44 P. M. Sirimanne, M. Rusop, T. Shirata, T. Soga and T. Jimbo, *Mater. Chem. Phys.*, 2003, **80**, 461.

45 K. Ravichandran, R. Anandhi, K. Karthika, P. V. Rajkumar, N. Dineshbabu and C. Ravidhas, *Superlattices Microstruct.*, 2015, **83**, 121.

46 C. Li, F. Wang, J. Xu, J. Yao, B. Zhang, C. Zhang, M. Xiao, S. Dai, Y. Li and Z. a. Tan, *Nanoscale*, 2015, **7**, 9771.
47 S. Inudo, M. Miyake and T. Hirato, *Phys. Status Solidi A*, 2013, **210**, 2395.
48 K. Liang, D. B. Mitzi and M. T. Prikas, *Chem. Mater.*, 1998, **10**, 403.
49 N. J. Jeon, J. H. Noh, Y. C. Kim, W. S. Yang, S. Ryu and S. I. Seok, *Nat. Mater.*, 2014, **13**, 897.
50 J. C. Bernede, L. Cattin, M. Makha, V. Jeux, P. Leriche, J. Roncali, V. Froger, M. Morsli and M. Addou, *Sol. Energy Mater. Sol. Cells*, 2013, **110**, 107.
51 S. Shao, J. Liu, J. Zhang, B. Zhang, Z. Xie, Y. Geng and L. Wang, *ACS Appl. Mater. Interfaces*, 2012, **4**, 5704.

# Table of contents

Low-cost solution-processed copper iodide replaces PEDOT:PSS in inverted planar heterojunction perovskite solar cells with high efficiency and enhanced stability.